MOTION OF GLACIERS, SEA ICE, AND ICE SHELVES IN CANISTEO PENINSULA, WEST ANTARCTICA OBSERVED BY 4-PASS DIFFERENTIAL INTERFEROMETRIC SAR TECHNIQUE

Hyangsun Han and Hoonyol Lee*

Department of Geophysics, Kangwon National University
Hyoja-dong, Chuncheon, Kangwon-do 200-701
*Corresponding author (email: hoonyol@kangwon.ac.kr)

ABSTRACT: We have extracted a surface deformation map of a part of Canisteo Peninsula on Amundsen Sea in West Antarctica by applying 4-pass DInSAR technique to two ERS-1/2 tandem pairs obtained on October 21-22, 1995 (diff-pair) and March 9-10, 1996 (topo-pair), and analyzed changes of glaciers, sea ice, ice shelves, and their kinematic interactions. We observed fast motion of glaciers pushing the adjoining sea ice. Some interferometric phases indicate the up-rise of sea ice of which type is thought to be land-fast ice to exert repulsive force against the pushing glacier. There were other glaciers and sea ice that moved to the same direction, suggesting that the sea ice in these regions was land-fast ice weakly harnessed to sea bottom or pack ice not harnessed at all. Several small circular fringes in ice shelves suggested that islands or seamounts on the bottom of ice shelves deterred the movement of ice shelves, resulting in the rise of ice surface.

KEY WORDS: ERS-1/2, Glaciers, Sea ice, Ice shelves, 4-pass DInSAR

1. INTRODUCTION

Glaciers, sea ice, and ice shelves are closely related to the global warming and sea level rising. In the Arctic, the lowest latitude of marginal ice zones goes up every years and a rapid decrease in glaciers and ice shelves at Greenland is distinctly observed. The motion of glaciers and the degradation of ice shelves in the Antarctic is being accelerated (Rignot *et al.*, 2005).

The glaciers and ice shelves in the West Antarctica are decreasing more quickly than other regions in Antarctica. Ice shelves in the region diminish in bulk by 65 km^3 per year resulting in the rise of sea level by 0.16 mm per year (Thomas *et al.*, 2004). Considering the decrement in all of the glaciers and ice shelves in West Antarctica, sea level rising amounts to 0.2 mm per year. Rignot (1998) investigated the hinge line of Pine Islands Glacier by applying interferometric method to ERS-1/2 SAR (Synthetic Aperture Radar) images. According to the investigation, the hinge line moved back about 1.2 km between 1992 and 1996, and the thickness of the glacier was thinned by 3.5 m per year.

SAR interferometry (InSAR) uses the difference of phases between two or more SAR images of same area. InSAR has been widely used to extract topography and deformation of the surface. Differential SAR interferometry (DInSAR) is the method to extract displacement of surface by removing topographic phases using digital elevation model (DEM) or other interferogram. DInSAR technique was applied to measure displacements by earthquake (Yen *et al.*, 2008), volcano (Lagios *et al.*, 2005), ground subsidence (Tomás *et al.*, 2005), motion pattern of glaciers (Cheng and Xu, 2006; Rignot, 1998) and ice shelves (Kwoun *et al.*, 2005).

In this study, we used ERS-1/2 SAR images to observe the changes of glaciers, sea ice, and ice shelves in Canisteo Peninsula, West Antarctica. We extracted interferometric phases from ERS-1/2 tandem pairs obtained on October 21-22, 1995 and March 9-10, 1996, analyzed the motion of glaciers, sea ice, ice shelves, and their kinematic interactions by using 4-pass DInSAR technique.

2. STUDY AREA AND DATA

Canisteo Peninsula is located near Amundsen Sea in West Antarctica. The width and length of the peninsula are about 40.6 km and 56.3 km, respectively (Fig. 1). Ice shelves and small islands exist around the peninsula. There are several glaciers of different size on the coastal area and the crevasses are developed between the peninsula and ice shelves. The entire area is covered with snow and ice at all times whereas the exposed base rocks are limited to some islands. The ocean surrounding the peninsula opens in summer and is filled with variety types of sea ice in other seasons.

We used ERS-1/2 tandem pairs over the Canisteo Peninsula obtained on October 21-22, 1995 and March 9-10 1996. October is Antarctic springtime when sea ice begins to melt slowly. Fig. 1 is ERS-1 SAR image obtained on 21 October, 1995. A large portion of the ocean is covered with flat sea ice widely distributed near the coastline. Table 1 shows ERS-1/2 tandem pairs used in this study and the associated information.

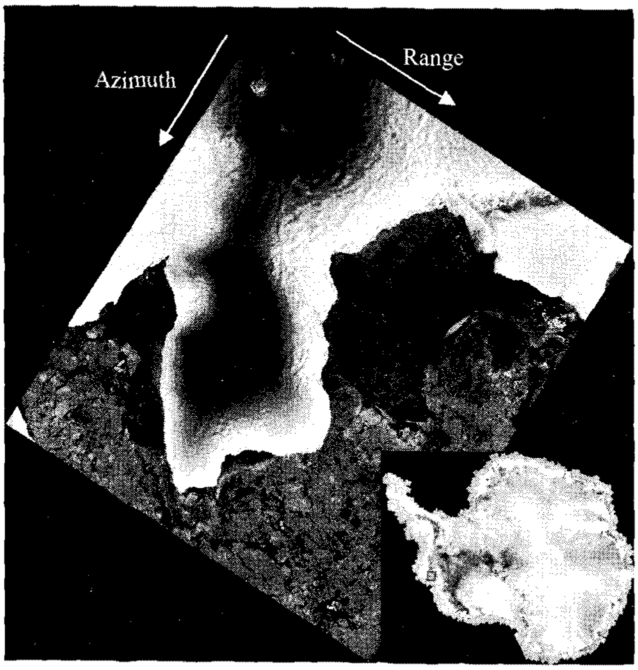

Fig. 1. Geocoded ERS-1 SAR image of the study area (October 21, 1995, 100 km x 100 km). The Canisteo Peninsula is located in the West Antarctica (small red box on the left lower image).

Table 1. ERS-1/2 tandem pairs used in this study.

Track	Orbit (ERS-1/2)	Date	*Bperp (m)	*Ha (m)
278	22310/ 2637	1995/10/21 1995/10/22	40.0	243.2
	24314/ 4641	1996/03/09 1996/03/10	152.4	63.9

*Bperp: perpendicular baseline
*Ha: Height ambiguity

3. METHOD

For the 2-pass DInSAR, an accurate digital elevation model over the study area is needed. The best DEM available for the West Antarctica is the Radarsat-1 Mapping Project (RAMP) DEM (Kwoun *et al.*, 2005) However the RAMP DEM is not accurate enough to apply 2-pass DInSAR in this study because it has the horizontal resolution of 400 m in this region (Liu *et al.*, 1999). We used 4-pass DInSAR technique that can extract surface displacement without pre-existing DEM. The 4-pass DInSAR uses one interferogram to estimate the topographic phases (topo-pair) to be subtracted from the other interferogram containing the phases of deformation (diff-pair).

There are several steps for the interferogram generation. The first step is the generation of single look complex (SLC) images from the RAW data. The range and azimuth offsets between two SLC images are then calculated and the two images are co-registered. The two co-registered SLC images are used to generate multi-look interferogram. Next, the interferometric baseline is computed from state vectors, and then the phase trend by earth ellipsoid is removed from interferogram (earth-flattening). Finally, the earth-flattened interferogram is generated.

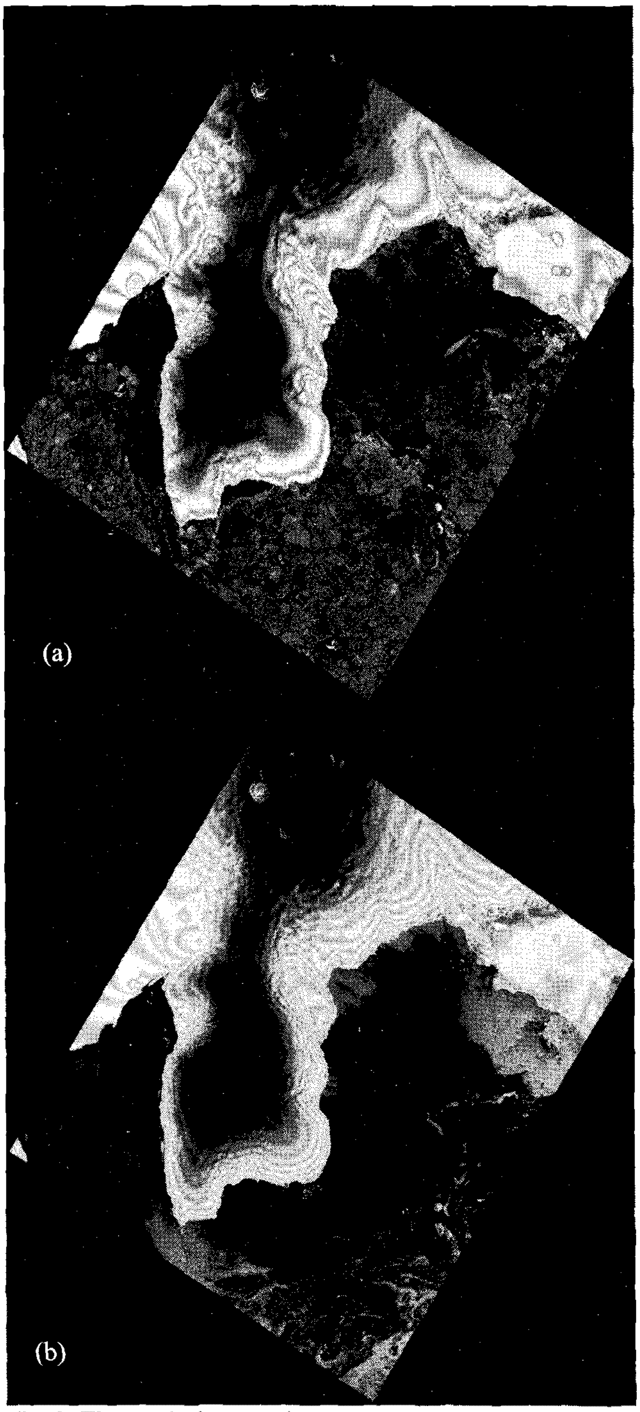

Fig. 2. The earth-flattened interferograms extracted from the diff-pair (a) and topo-pair (b). (a) shows displacement phase of glaciers, sea ice, and ice shelves with some topographic phase whereas (b) shows topographic phases with little displacement phase.

Coherence in the two ERS-1/2 tandem pairs used in this study was well maintained so that we could make the interfeorgrams. The baseline of the tandem pair obtained on October 21-22, 1995 is about 40 m and the height ambiguity of a topographic fringe is 243.2 m. October is springtime and many changes occur over the surface. The baseline, height ambiguity, and season of this pair are suitable for observation of the deformation, and so we used it as a diff-pair. The other tandem pair was obtained on March 9-10, 1996 when all of the sea ice disappeared. The baseline and height ambiguity of this pair are about 152 m and 63.9 m, respectively. In the Antarctic, more surface changes occur in March than October due to the high temperature. However, we used this pair as a topo-pair because the baseline and height ambiguity is appropriate for extraction of the topographic phases.

Fig. 2 is the earth-flattened interferograms extracted from the diff-pair (Fig. 2a) and topo-pair (Fig. 2b). There is a gap of 5 months between the two pairs. The fringes on the surface of glaciers and sea ice are remarkably displayed and many circular fringes on ice shelves are observed in the diff-pair interferogram. These fringes are not the effects of topography. There are no fringes on some sea ice because of large movement of sea ice during a day. In the topo-pair interferogram, the topographic phases are well displayed rather than displacement phases.

We have determined diff-pair and topo-pair as above, but there remain some weaknesses and limitation. The topo-pair is obtained on March when is the summertime of the Antarctic. Snow and ice in the Antarctic decrease rapidly and the deformations arise from it. Although the topo-pair interferogram well shows topographic phases, there should be some phases of deformations in the interferogram as well.

4. ANALYSIS OF DIFFERENTIAL INTERFEROGRAM

Fig. 3 is the earth-flattened and topography-removed interferogram. The major parts of topography over the peninsula were removed and the fringes by deformation were shown in the differential interferogram. One fringe in the differential interferogram represents the change of 2.83 cm from radar to ground.

Region (a) includes the largest glacier in this region moving toward the sea ice about 14.2 cm whereas the sea ice shows up rise interferometric phases. The pushing glacier gave repulsive force to sea ice of which type is thought to be land-fast ice, and then the land-fast ice showed a sort of the structure of an anticline. Similar kinematic structures are found in some other glaciers and sea ice in this study area. In region (b), the glacier rapidly moved to land-fast ice and the interferometric phases of the adjoining land-fast ice indicated the up rise of sea ice surface.

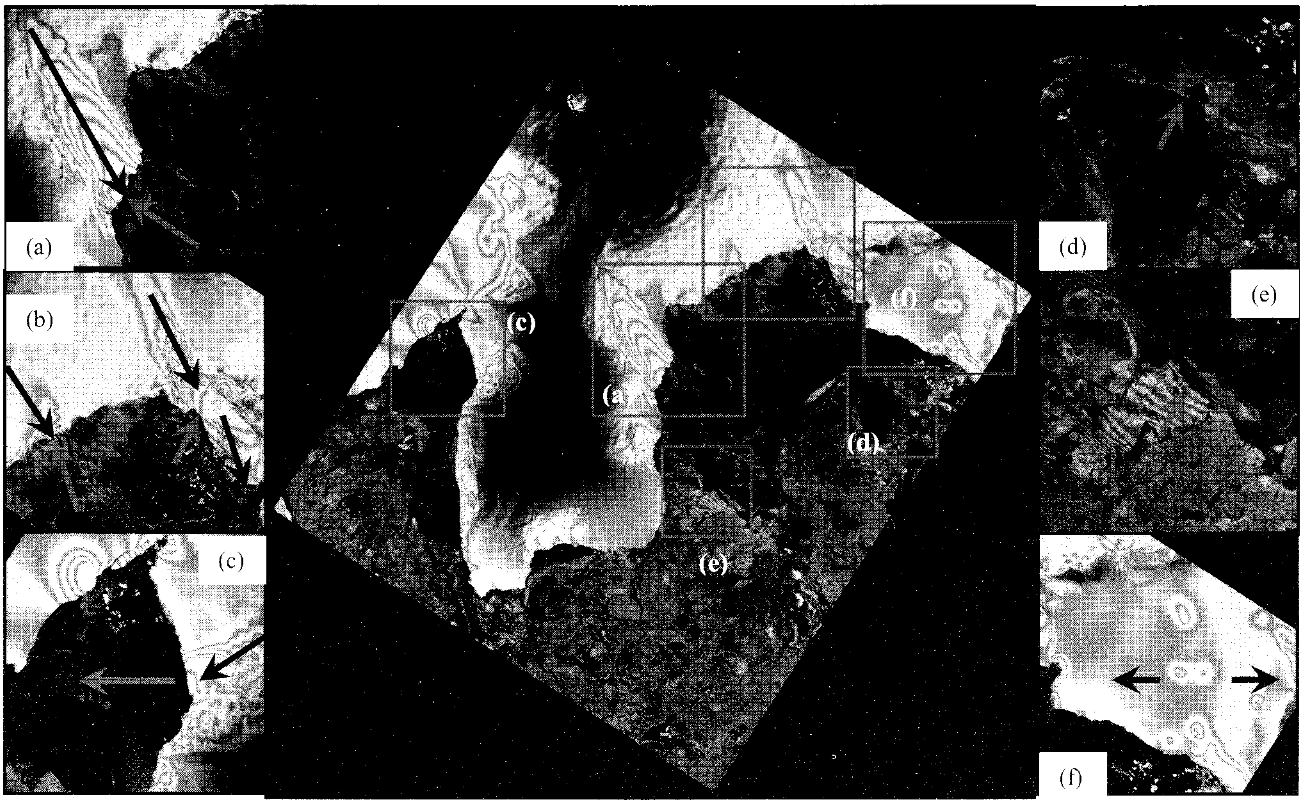

Fig. 3. The differential interferogram of the study area. One fringe (from purple to yellow, cyan, and purple again) in the differential interferogram represents the decrease of range by 2.83 cm from radar to target. Region (a) and (b) shows fast motion of glaciers pushing adjoining sea ice. Glacier and sea ice moved to the same direction in region (c). Sea ice showed fast motion in region (d) and (e). In region (f), there are many circular fringes observed on the ice shelf.

In region (c), glacier and sea ice show interferometric phases of the same direction. It is thought that the sea ice was being moved by the motion of glacier in the same horizontal direction towards the sea. The surface morphology of sea ice in this region is similar to that of land-fast ice, however considering the motion of glacier and sae ice, it was suggested that the ice type is the land-fast ice weakly harnessed to sea bottom or pack ice not harnessed at all.

Region (d) and (e) are the pack ice showing rapid motion driven by ocean tide. Region (f) shows many circular interferometric phases on ice shelves. They are observed in both the topo-pair and diff-pair interferogram. Considering there are many islands around the Canisteo Peninsula, seamounts or unidentified islands may be under the bottom of the ice shelves and caused the motion on the surface of ice shelves.

5. CONCLUSION

The 4-pass DInSAR technique applied to ERS-1/2 Tandem pairs of Canisteo Peninsula, West Antarctica revealed dynamic features of glaciers, sea ice and ice shelves, and their interactions. We saw the upwelling sea ice by repulsive force against the fast motion of glacier. We can also determine the type of sea ice to be land-fast. Sea ice showing the movement in the same direction with the sliding glaciers could be land-fast ice weakly connected to sea bottom or pack ice that is not connected at all. In the edge of land-fast ice, we observed rapid motion of sea ice, which makes a clear boundary between land-fast ice and pack ice. The circular fringes on the ice shelves were caused by unidentified islands or seamounts at the bottom of ice.

Through this study, we could analyze the interaction between glaciers and sea ice, decide the sea ice types and conditions between different ice types, and analyze the topography underneath ice shelves.

For more detailed analysis on the dynamic relationships between glaciers, sea ice, and ice shelves, it is necessary to apply numerical analysis and modelling which remain as the subject of ongoing study.

REFERENCE

Cheng, X. and Guanhua, X., 2006. The integration of JERS-1 and ERS SAR in differential interferometry for measurement of complex glacier motion, *Journal of Glaciology*, 52(176), pp. 80-88.

Kwoun, O., Baek, S., Lee, H., Sohn, H., Han, U., and Shum, C. K., 2005. Topography, vertical and horizontal deformation in the Sulzberger Ice Shelf, West Antarctica using InSAR, *Korean Journal of Remote Sensing*, 21(1), pp. 73-81.

Lagios, E., Sakkas, V., Parcharidis, I., and Dietrich, V., 2005. Ground deformation of Nisyros Volcano (Greece) for the period 1995-2002: Result from DInSAR and DGPS observations, *Bulletin of Volcanology*, 68(2), pp. 201-214.

Liu, H., Jezek, C. K., and Li, B., 1999. Development of an Antarctic digital elevation model by integrating cartographic and remotely sensed data: A geographic information system based approach, *Journal of Geophysical Research*, 104(B10), pp. 23,199-23,213.

Tomás, R., Márquez, Y., Lopez-Sanchez, J. M., Delgado, J., Blanco, P., Mallorquí, J. J., Martínez, M., Herrera, G., and Mulas, J., 2005. Mapping ground subsidence induced by aquifer overexploitation using advanced Differential SAR Interferometry: Vega Media of the Segura River (SE Spain) case study, *Remote Sensing of Environment*, 98(2), pp. 269-283.

Thomas, R., Rignot, E., Casassa, G., Kanagaratnam, P., Acuña, C., Akins, T., Brecher, H., Frederick, E., Gogineni, P., Krabill, W., Manizade, S., Ramamoorthy, H., Rivera, A., Russell, R., Sonntag, J., Swift, R., Yungel, J., and Zwally, J., 2004. Accelerated sea-level rise from West Antarctica, *Science*, 306, pp. 255-258.

Rignot, E. J., 1998. Fast recession of a west Antarctic glacier, *Science*, 281, pp. 549-551.

Rignot, E., Casassa, G., Gogineni, S., Kanagaratnam, P., Krabill, W., Pritchard, H., Rivera, A., Thomas, R., Turner, J., and Vaughan, D., 2005. Recent ice loss from the Fleming and other glaciers, Wordie Bay, West Antarctic Peninsula, *Geophysical Research Letters*, 32, L07502, doi:10.1029/2004GL021947.

Yen, J., Chen, K., Chang, C., and Boerner, W., 2008. Evaluation of earthquake potential and surface deformation by Differential Interferometry, *Remote Sensing of Environment*, 112(3), pp. 782-795.